RESEARCH ARTICLE

Toplayer-dependent crystallographic orientation imaging in the bilayer two-dimensional materials with transverse shear microscopy

Sabir Hussain[1,2,4,*], Rui Xu[1,*], Kunqi Xu[3], Le Lei[1], Shuya Xing[1], Jianfeng Guo[1], Haoyu Dong[1], Adeel Liaqat[2,4], Rashid Iqbal[2,4], Muhammad Ahsan Iqbal[2,4], Shangzhi Gu[1], Feiyue Cao[1], Yan Jun Li[5], Yasuhiro Sugawara[5], Fei Pang[1], Wei Ji[1], Liming Xie[2,4], Shanshan Chen[1,†], Zhihai Cheng[1,‡]

1*Beijing Key Laboratory of Optoelectronic Functional Materials & Micro-nano Devices, Department of Physics, Renmin University of China, Beijing 100872, China*
2*CAS Key Laboratory of Standardization and Measurement for Nanotechnology, CAS Center for Excellence in Nanoscience, National Center for Nanoscience and Technology, Beijing 100190, China*
3*Key Laboratory of Inorganic Functional Materials and Devices, Shanghai Institute of Ceramics, Chinese Academy of Sciences, Shanghai 200050, China*
4*University of Chinese Academy of Sciences, Beijing 100039, China*
5*Department of Applied Physics, Graduate School of Engineering, Osaka University, 2-1 Yamadaoka, Suita, Osaka 565-0871, Japan*
Corresponding authors. E-mail: †schen@ruc.edu.cn, ‡zhihaicheng@ruc.edu.cn
Received February 17, 2021; accepted April 19, 2021

Supporting Information

Materials and Methods

Chemical vapor deposition (CVD)-grown MoS_2 on amorphous SiO_2/Si substrate: The MoS_2 layers were grown on 200nm SiO_2/Si supporting substrate by CVD method. MoO_3 (99.5% purity) and Sulfur (99.5% purity) were used as the precursor and reactant, respectively. MoO_3 powder (25mg) was placed in a quartz boat at the center of a furnace. The SiO_2/Si substrate (2×2 cm^2) was carefully place face down above the MoO_3 powder. The sulfur powder was heated to 180°C and was carried through Ar gas flow at 500sccm. The experiment was conducted at a reaction temperature ~750°C.

Chemical vapor deposition (CVD)-grown MoS_2 on atomically flat crystalline Al_2O_3 substrate: Put MoO_3 and S_2 powder in the designed powder. The MoO_3 powder is placed at the heating center, and the S powder is placed at a position about 17cm upstream from the MoO_3 powder. The atomically flat crystalline (Al_2O_3) supporting substrate is placed about 0.5cm above the MoO_3 powder, with polished side down. There is large amount of S powder, which can probably can cover the entire the bottom of the porcelain boat. The MoO_3 powder only needs a small particle visible to the nacked eye (0.01mg level). After placing the porcelain boat, immediately encapsulate the same gas, and then turn on the powder for heating. Heating conditions: heating to 870°C for 25-30 minutes from room temperature, then constant temperature at 870°C for 5 minutes, then natural cooling to room temperature. Gas: A mixture of 90% Ar and 10% H_2 has a flow rate of 35sccm.

CVD-grown bilayer Graphene on amorphous SiO_2/Si substrate: A Low-pressure CVD system was used for the growth of bilayer graphene on flat Cu foil. Typically, the Cu foil (Alfa Aesar, 25μm, 99.8%) was electropolished to smooth the surface as well as to remove the coating layer typically applied by the manufacturer. Then the pre-treated Cu foil was loaded into the reaction chamber of the quartz tube furnace. The CVD system was evacuated and heated up to 1030℃ in 20sccm H_2 and held for another 30min to anneal the copper foil. After annealing, the growth was carried out with a 1.5 sccm methane flow for 1min followed by a 1sccm methane flow for another 20min. The hydrogen flow was maintained at 20sccm during the growth and the cooling process. After growth, the graphene film was transferred onto the amorphous SiO_2/Si substrate through the typical Polymethyl methacrylate (PMMA) assisted wet etching process.[4]

Optical microscopy: Optical characterization of MoS_2 layers was conducted by optical microscopy (ECLIPSE LV150N, Nikon).

Atomic force microscopy (AFM) measurements: All the AFM measurements were performed under ambient condition (MFP-3D Infinity, Asylum Research). The following functional AFM modes were used in this study:
Transverse shear microscopy (TSM) and friction force microscopy (FFM): TSM and FFM are the derivatives of contact mode of AFM, which is optimized to measure the torsion signal between the tip and sample surface. For FFM, the scan direction of the AFM tip is perpendicular to the long axis of the AFM cantilever, and then the friction property of the sample was obtained by detecting the torsion signal of the cantilever. For TSM, the scan direction of the AFM tip is parallel to the long axis of the cantilever, and then the shear property of the sample was obtained by detecting the torsion signal of the cantilever. Both strain applied by substrate and induced by probe will enhance the TSM signal. All the FFM and TSM measurements were performed with a sharp Silicon AFM probe (AC160, Asylum Research) with spring constant of 22.2N/m was used over the course of investigation, with the scanning speed 1.5m/s.
Kelvin probe force microscopy (KPFM): KPFM measurements were carried out at room temperature. Commercially available conductive tip (conductive Pt/Ir coated AFM tip). KPFM measurements were recorded simultaneously AFM images with using the standard two-pass techniques: the first pass used to record the topographic images. Meanwhile second pass used to record the surface potential mappings by keeping the tip at selected the tip height with respect to recorded the topographic image. In our study the electrical tip was kept at a left height at 50nm to avoid the topographic artifacts.

S1. Anisotropic response in merging flakes

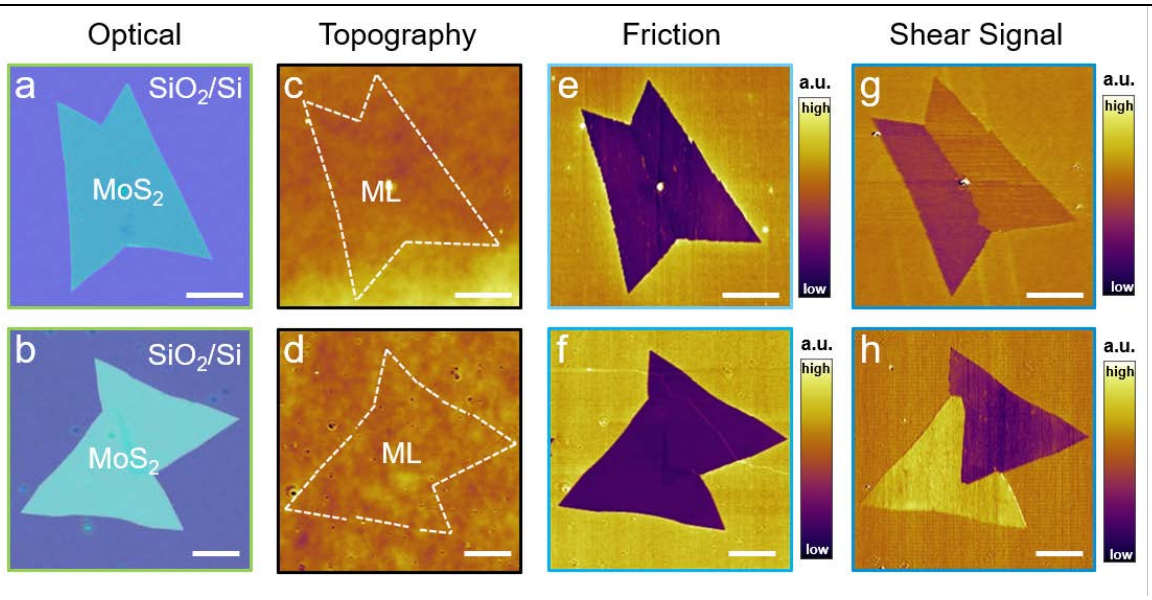

Fig. S1 (a, b) Optical, **(c, d)** topographic, **(e, f)** FFM and **(g, h)** TSM measurement of two typical MoS_2 merging flakes. Their different crystallographic orientations were clearly determined by the shear signal of TSM measurements.[1] The scale bars are all 5μm.

S2. Loading force dependent imaging by TSM and FFM

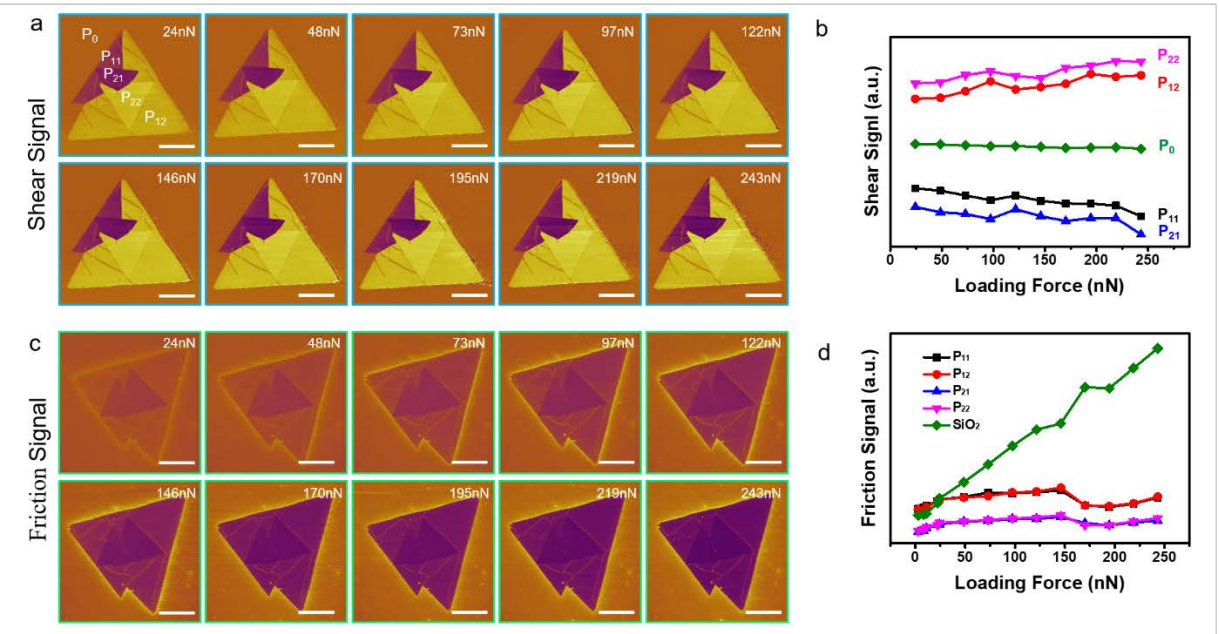

Fig. S2 The *in-situ* TSM and FFM Characterizations with the increasing loading forces of AFM tip. **(a)** TSM images under different loading force. **(b)** The profile lines illustrate shear signals vs loading force. **(c, d)** FFM images under different loading force and corresponding profile lines. The scale bars are all 8μm.

We employed the load dependent TSM and FFM techniques to characterize the bilayer MoS_2/SiO_2. Fig. S2a and S2b illustrate the nanomechanical contact response's signals and friction signals corresponding their loading forces. It can be seen that in profile line S2b and S2d the load dependent force can regulate the out of plan elastic deformation and friction response. Since it increases the contact area between the AFM tip and the sample surface, create a more puckered geometry and friction. Thus, the higher the loading force cause the higher stretch deformation and higher friction. During the low loading force, the contrast between the monolayer and bilayer is minimal, but at as the loading force increased cause the contrast grows as shown in figure S2(b). Fig. S2b illustrate the stretch deformation, where the brighter contrast has higher stretch deformation.[2, 3] According to our earlier work, the friction force is nearly proportional to the magnitude of the deformation.[1] For FFM, Fig. S2d illustrate the friction profile according to the load dependent by AFM tip from initiation to saturation point.

S3. TSM images of multi-grain graphene films directly on the growth Copper substrate

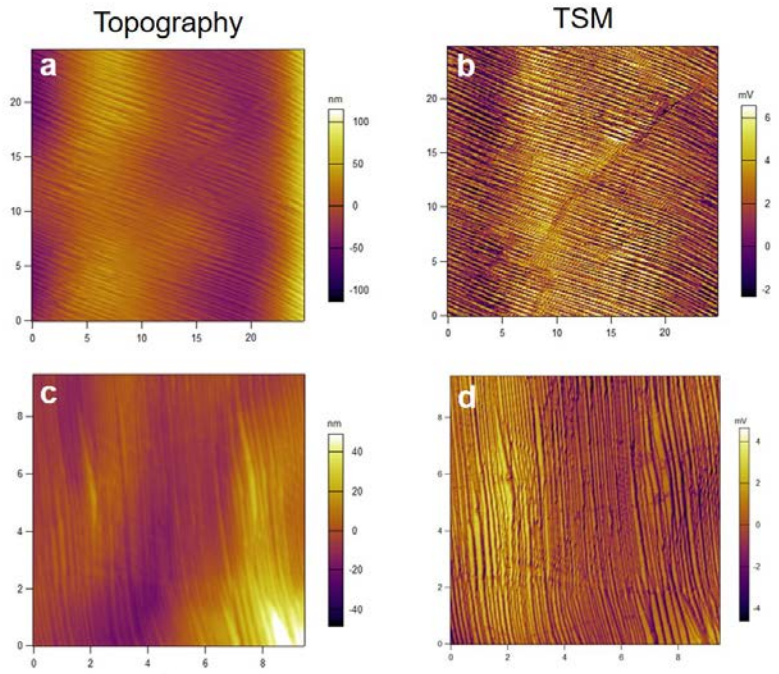

Fig. S3 (a, c) AFM topography and **(b, d)** TSM images of multi-grain graphene films directly on the growth Copper substrate. Different from the transfer graphene on the SiO_2/Si substrate, no grains were observed within the films, which should be due to the strong bonding between the 2D samples and substrates.

References

1. K. Xu, Y. Pan, S. Ye, L. Lei, S. Hussain, Q. Wang, Z. Yang, X. Liu, W. Ji, R. Xu, and Z. Cheng, *Appl. Phys. Lett.* 115(6), 063101 (2019)
2. Z. Ye, A. Balkanci, A. Martini, and M. Z. Baykara, *Phys. Rev. B* 96(11), 115401 (2017)
3. S. Li, Q. Li, R. W. Carpick, P. Gumbsch, X. Z. Liu, X. Ding, J. Sun, and J. Li, *Nature* 539(7630), 541 (2016)
4. H. Ying, W. Wang, W. Liu, L. Wang, and S. Chen, *Carbon* 146, 549 (2019)